Toxicon 55 (2010) 145–152

Contents lists available at ScienceDirect

Toxicon

journal homepage: www.elsevier.com/locate/toxicon

Silica coating magnetic nanoparticle-based silver enhancement immunoassay for rapid electrical detection of ricin toxin

Jie Zhuang [a,d], Tao Cheng [b], Lizeng Gao [a], Yongting Luo [a,d], Quan Ren [b], Di Lu [a], Fangqiong Tang [c], Xiangling Ren [c], Dongling Yang [a], Jing Feng [a], Jingdong Zhu [a], Xiyun Yan [a,*]

[a] National Laboratory of Biomacromolecules, Institute of Biophysics, Chinese Academy of Sciences, 15 Datun Road, Beijing 100101, China
[b] Institute of Electrical Engineering, Chinese Academy of Sciences, Beijing 100090, China
[c] Laboratory of Organic Optoelectronic Functional Materials and Molecular Engineering, Technical Institute of Physics and Chemistry, Chinese Academy of Sciences, Beijing 100080, China
[d] Graduate School of the Chinese Academy of Sciences, Beijing 100049, China

ARTICLE INFO

Article history:
Received 19 March 2009
Received in revised form
13 July 2009
Accepted 14 July 2009
Available online 23 July 2009

Keywords:
Magnetic nanoparticles
Gold nanoparticles
Interdigitated array microelectrodes
Ricin detection

ABSTRACT

We developed a novel silica coating magnetic nanoparticle-based silver enhancement immunoassay (SEIA) for ricin toxin (RT) rapid electrical detection using interdigitated array microelectrodes (IDAMs) as electrodes. This novel system was developed by taking advantage of the separation and enrichment properties of magnetic nanoparticles (MNPs) and the catalytic properties of gold nanoparticles (GNPs). In this system, MNPs labeled with anti-ricin A chain antibody 6A6 were used to capture ricin and GNPs labeled with anti-ricin B chain antibody 7G7 were used as detectors. To enhance the electrical signal, the catalytic properties of GNPs were used to promote silver reduction. In the presence of ricin, a sandwich structure was formed which could be separated by a magnetic field. The sandwich complex was then transferred to IDAMs. The silver particles bridged the IDAM gaps and gave rise to an enhancing electrical signal that was detected by conductivity measurements. The results showed that the sensitivity of the SEIA for ricin electrical detection was five times greater than that of conventional colorimetric sandwich ELISA. Once the antibody used for detection was coated on the plates or MNPs, our system was three times more rapid than colorimetric sandwich ELISA. This rapid and sensitive detection system provides promising new potential for ricin detection.

1. Introduction

Ricin is one of the most toxic and easily obtainable plant toxins and is isolated from the seeds of castor bean *Ricinus communis* (Roberts and Smith, 2004). The ricin toxin is a heterodimer comprised of a 32 kDa A chain and a 34 kDa B chain connected by interchain disulfide bonds (Stine et al., 2005). The B chain is a lectin which binds specifically to galactosyl residues on the cell surface and appears to trigger the endocytic uptake of ricin. The A chain is separated from the B chain in the cytoplasm and enzymatically inactivates the 60S ribosomal subunit, disrupting protein synthesis. Ricin is the only protein toxin listed under the Schedule 1 category of the Chemical Weapons Convention (CWC) (Atlas, 2002). Intake of trace amounts of ricin results in diarrhea, vomiting, septic shock, pyrogenicity, and even death. The U.S. Centers for Disease Control (CDC) gives a possible minimum amount of 500 μg for the lethal dose of ricin for humans if exposure is from injection or inhalation. Therefore, it is important to be able to detect

* Corresponding author. National Laboratory of Biomacromolecules, Institute of Biophysics, Chinese Academy of Sciences, 15 Datun Road, Beijing 100101, China. Tel.: +86 10 6488 8583; fax: +86 10 6488 8584.
E-mail address: yanxy@sun5.ibp.ac.cn (X. Yan).

0041-0101/$ – see front matter © 2009 Elsevier Ltd. All rights reserved.
doi:10.1016/j.toxicon.2009.07.015

ricin in food and water. Conventional analytical methods including radioimmunoassay (Godal et al., 1981), enzyme-linked immunosorbent assay (ELISA) (Poli et al., 1994), fluorescence-based fiber optic immunoassay (Narang et al., 1997) aptamer microarrays (Kirby et al., 2004), mass-sensitive biosensor (Tran et al., 2008), micro-electrochemical biosensors (Guglielmo-Viret and Thullier, 2007) and electrochemiluminescent (ECL) assay (Garber and O'Brien, 2008) are effective for ricin detection. However these analytical methods are time-consuming and therefore not suitable for biodefense. Therefore, it is important to develop a rapid method for detection of trace amounts of ricin.

The development of immunoassays during the last four decades has revolutionized the determination of clinical cancer markers as well as contaminants in the environment area. There are various methods for analyte measurement including optical, mass-sensitive, thermal and electrochemical detections (Fang et al., 2008). Among these, the optical biosensors are the most studied, but the detection limits are expected to be better for the electrochemical sensors and the instruments are less complicated and suitable for disposable assays (Berggren et al., 2001). Electrochemical biosensors are further classified as amperometric, potentiometric and conductometric biosensors (Berggren et al., 2001). With increased necessity for rapid detection assays in recent times, conductometric biosensors have been applied in various biological and biomedical sciences, which measure electrical resistance as their signal readout. Interdigitated array microelectrodes (IDAMs) have been developed because they have improved sensitivity compared with common electrodes (Varshney and Li, 2007, 2008). Combining resistance measurements with IDAMs should greatly enhance target detection sensitivity and simplify the fabrication and operational requirements.

Gold nanoparticles (GNPs) are more sensitive and selective than conventional probes in a variety of biodetection schemes (Elghanian et al., 1997; Taton et al., 2000). They have cooperative binding properties, unique optical properties, and catalytic properties, including the promotion of silver reduction reactions that have been used in systems to amplify electrochemical signals (Taton et al., 2000). Magnetic nanoparticles (MNPs) are of particular interest because of their power in biological imaging and separation techniques (Taton et al., 2001), and have been used for separating proteins, DNA and cells (Gu et al., 2006; Hoshino et al., 2007), for drug and gene targeting (Alexiou et al., 2007), for magnetic resonance imaging (Chertok et al., 2008), and for magnetic biosensors (Chemla et al., 2000). Several new ultrasensitive protein detection methods taking advantage of the properties of both MNPs and GNPs have been developed. For example, a novel immunoassay, named the gold fluorescence-quenching immunoassay (GFQIA), has been developed using the fluorescence-quenching property of GNPs, and has been used for AFP detection (Ao et al., 2006) and an Au^{3+}-catalyzed chemiluminescent metal immunoassay (CLMIA) based on Au^{3+} release after oxidative GNP dissolution has been used for IgG detection (Fan et al., 2008). However, both GFQIA and CLMIA do not make use of the intrinsic catalytic properties of GNPs which can lead to a five orders of magnitude improvement in the sensitivity of detection (Taton et al., 2000). CurrentlyHill et al. (2007) have reported a bio-barcode detection system which involved MNPs and GNPs. But these systems require another chip-based detection method which sophisticated the procedure for detection. It would be beneficial if one can obviate or minimize the schemes without sacrificing the ultrasensitivity of the bio-barcode assay.

Recently we have found that MNPs possess intrinsic peroxidase-like activity that can catalyze oxidation of various peroxidase substrates such as hydroquinone (Gao et al., 2007). This property of MNPs could potentially cause a high background in immunoassays combining the separation properties of MNPs and the catalytic properties of GNPs, thus limiting detection sensitivity. Interestingly, we previously found that coating MNPs with silica shields their intrinsic peroxidase activity and should thus eradicate this limitation. Here we combine the catalytic properties of GNPs with the separation properties of silica coating MNPs without peroxidase activity, to assemble a SEIA for ricin electrical detection. Compared with conventional colorimetric sandwich ELISA using the same pair of antibodies, SEIA using IDAMs as electrodes was more sensitive and rapid for electrical detection of ricin.

2. Materials and methods

2.1. Reagents

Tetraethoxysilane (TEOS), 3-aminopropyltriethoxysilane (APTES), *N*,*N*-dimethylformamide (DMF), $HAuCl_4$, 1-ethyl-3-(3-dimethyl-aminopropyl) carbodiimide (EDC), *N*-hydroxysuccinimide (NHS) and Silver Enhancement Kit solution were purchased from Sigma–Aldrich. $Na_3C_6H_5O_7$, $FeCl_3 \cdot 6H_2O$, ethylene glycol were from Beijing Chemical Reagents. Bradford protein concentration assay was from Bio-Rad. Horseradish peroxidase (HRP)-labeled goat anti-mouse IgG was provided by Santa Cruz. ECL (Enhanced Chemiluminescence) substrate solution was obtained from Pierce. Purified ricin toxin (RT) and recombined ricin toxin A chain (RTA) were kindly provided by Prof. Beifen Shen.

2.2. Production of anti-ricin monoclonal antibodies

Using ricin as immunogen, anti-ricin antibodies were raised in *Balb/c* mice using a procedure previously described (Kohler and Milstein, 1975). Briefly, after immunization, the mouse with the highest titer was selected for preparation of mAbs. Spleen cells from the mouse were fused with NS1 mouse myeloma cells, and specific anti-ricin antibodies in myeloma culture supernatants were detected using ELISA.

2.3. ELISA

Polystyrene plates were coated with 5 μg/ml purified ricin in 0.05 M $NaHCO_3$ (pH 9.6) at 4 °C overnight, and washed three times with PBS containing 0.05% (v/v) Tween-20 (PBST). Unbound sites were blocked with 3% (w/v) bovine serum albumin (BSA) at 37 °C for 1 h.

Antibodies at a concentration of 1 μg/ml were added and incubated at 37 °C for 1 h. After washing with PBST, horseradish peroxidase (HRP)-labeled goat anti-mouse IgG was added and incubated at 37 °C for 45 min. Plates were washed a further three times with PBST, and peroxidase activity was then measured with TMB substrate solution. After incubation at room temperature for 5 min, the reaction was stopped by the addition of 2 M H_2SO_4. The absorbance of each well at 450 nm was determined.

2.4. Colorimetric sandwich ELISA

Polystyrene plates were coated with 2 μg/ml purified capture antibody in 0.01 M PB at 4 °C overnight, and then washed three times with PBS containing 0.05% (v/v) Tween-20 (PBST). Unbound sites were blocked with 3% (w/v) BSA at 37 °C for 1 h. Ricin at a series of dilutions (from 2 nM to 5 pM) and PBS as negative control were added and incubated at 37 °C for 1 h. After washing with PBST, 1 μg/ml detection antibody labeled with biotin was added and incubated at 37 °C for 1 h. Plates were washed again three times with PBST, and HRP-conjugated avidin was then added and incubated at 37 °C for 1 h. Peroxidase activity was measured with TMB substrate solution. After incubation for 5 min at room temperature, the reaction was stopped by addition of 2 M H_2SO_4. The absorbance of each well at 450 nm was determined.

2.5. Western blotting

Ricin was reduced by 100 mM 1,4-dithiothreitol (DTT), then separated by 12% SDS-PAGE and blotted onto a nitrocellulose membrane. The membrane was blocked with 5% (w/v) milk in PBS at room temperature for 1 h and incubated with 1 μg/ml antibodies at room temperature for a further 1 h. After three washes with PBST, the membrane was incubated with the HRP-conjugated goat anti-mouse IgG for 1 h at room temperature. The membrane was washed again with PBST. ECL (Enhanced Chemiluminescence) substrate solution was added and the membrane was exposed to X-ray film to obtain optimal results.

2.6. Preparation of gold nanoparticle labeled anti-ricin antibodies

GNPs were prepared according to published methods (Oliver, 1994). In brief, all glassware used in the following procedure was cleaned in a bath of freshly prepared 3:1 HNO_3–HCl, rinsed thoroughly in deionized water and air dried. 1% (w/v) $HAuCl_4$ and 1% (w/v) $Na_3C_6H_5O_7$ were filtered using a 0.22 μm microporous membrane prior to use. GNPs were prepared by adding 2.5 ml 1% (w/v) $Na_3C_6H_5O_7$ to 100 ml boiling 1% (w/v) $HAuCl_4$, and stirring for 30 min. The color of the resulting solution changed from grey, to blue, purple, and then to wine red. The mixture was stirred for a further 10 min after removal from the heater. GNPs were stored in dark glass bottles at 4 °C for further use. The average size of GNPs obtained was 10 nm.

Detection antibodies were conjugated to GNPs. Anti-ricin A chain antibody 6A6 was purified using a Protein G column. The 10 μg purified antibody was then added to a pH-adjusted colloidal gold solution (pH 8.5). The mixture was allowed to stand for 10 min and then centrifuged at 12,000 *g* for 30 min. After centrifugation, gold pellets were blocked with 1% (w/v) BSA for 15 min. GNP probes were suspended in PBS, at an optical density of 5.0 at 520 nm.

2.7. Preparation of magnetic nanoparticle labeled anti-ricin antibodies

Amino group modified silica coating of MNPs was performed using an improved Ströber method which produces a relatively thick silica shell, as described by Yang et al. (2004). 26 mg Fe_3O_4 nanoparticles were mixed with 20 ml 2-propanol and 40 ml ethanol. 0.5 ml deionized water and 1.5 ml 25% (v/v) ammonia solution were added consecutively to the reaction mixture. Under continuous mechanical stirring, 100 μl APTES and 400 μl TEOS were added to the reaction solution.

Preparation of carboxy-group modified MNPs: 100 mg amino group modified silica coated MNPs were mixed with 50 mg glutaric anhydride and 5 ml DMF. The reactions proceeded at room temperature for 12 h in the dark.

MNPs were conjugated with capture antibodies. In brief, 50 μl of 50 mg/ml EDC, 50 μl of 50 mg/ml NHS, and 900 μl of deionized water were added to a vial and vortexed. Approximately 10 mg MNPs was dissolved in this solution and incubated at room temperature for 30 min. Nanospheres were collected using a magnet and washed twice with deionized water before adding to a solution containing 100 μl anti-ricin B chain antibody 7G7 (1 mg/ml), and 900 μl of NaAc (pH 6.0, 0.2 M). After vortexing, this mixture was incubated at 4 °C for 2 h. Antibody-labeled MNPs were separated using a magnet and washed twice with PBS and incubated in Tris solution (50 mM, pH 7.5) at room temperature for 30 min. Antibody-labeled MNPs were finally dispersed in 1 ml of PBS.

The antibody conjugation efficiency was determined using the Bradford protein concentration assay. The MNPs after being conjugated with antibody were removed with a magnet. The supernatant was centrifuged at 12,000 *g* for 5 min and further filtered using 0.22 μm filter to remove the MNPs remaining in supernatant.

2.8. Silver enhancement immunoassay

20 μg of capture antibody-coated MNPs was transferred into a 1.5 ml centrifuge tube and washed with 200 μl PBN buffer (phosphate buffer without sodium chloride). Subsequently, a series of dilutions of ricin (from 1 nM to 0.1 pM) were added and incubated at room temperature for 15 min with gentle stirring. The MNPs that had captured ricin were then separated with a magnet, and washed twice with 200 μl PBN buffer. 1.2×10^{15} particles/ml detection antibody-coated GNPs were added and the reaction was carried out at room temperature for 15 min. The MNPs separated by a magnetic field were washed with 200 μl PBN containing 0.05% (v/v) Tween-20 (PBNT), and 50 μl of the Silver Enhancement Kit solution (prepared by mixing solutions A and B 1:1) was added. The silver deposition reaction was carried out in solution for 5 min without stirring.

2.9. Instruments for electrical measurements

IDAMs used as electrodes were prepared by standard photolithography (Paguirigan and Beebe, 2007) and then washed with 0.1 M NaOH for 15 min, 0.1 M HCl for 15 min, acetone for 5 min and deionized water for 5 min, before immersion for 2 h in 2% (v/v) hexanethiol in ethanol to passivate the electrodes. Finally, the electrodes were washed with ethanol, followed by distilled water and were then dried under a stream of N_2. The resistance of each experiment was measured with a Fluke 189 multimeter (Fluke, Everett, WA). The difference of resistance in the presence and absence of ricin was taken as the signal produced by the immune reaction between mAbs and ricin.

3. Results and discussion

3.1. Principle for electrical detection of ricin toxin

A magnetic nanoparticle-based silver enhancement immunoassay (SEIA) for rapid electrical detection of ricin was designed as shown in Fig. 1. In this system, MNPs and GNPs were labeled with capture and detection antibodies respectively. A typical experimental procedure is as following: (A) Capture antibody-modified MNPs enriched ricin was separated using a magnetic field. (B) Detection antibody-modified GNPs recognized ricin separated by MNPs and sandwich structure was formed. (C) Then MNPs were separated using a magnet, and signal amplification was performed with silver ions which are reduced by hydroquinone to silver metal on the surface of the GNPs. (D) Electrical signal of Ag particles was evaluated with a Fluke 189 multimeter. In the presence of ricin, the binary nanoparticles (MNP–capture antibody–ricin–GNP–detection antibody) were formed and transferred to the IDAMs. There was a marked change of electrical signal, provided that enough Ag particles can fill the gaps of IDAMs. Oppositely, in the absence of ricin, only the naked MNPs did not cause electrical enhancement.

3.2. Characterization of anti-ricin monoclonal antibodies

To carry out a colorimetric sandwich ELISA for ricin sensitive detection, two antibodies recognized different epitopes of ricin were screened for their suitability as detection or capture antibodies (Hill and Mirkin, 2006). Six anti-ricin mAbs were produced by hybridoma technique. ELISA analysis showed that 6A6 and 7G7 had higher binding ability than the other four (Fig. 2A). Moreover, western blotting assay showed that 6A6 and 7G7 recognize different epitopes of ricin A chain (RTA) and B chain (RTB) respectively (Fig. 2B). Therefore we chose 6A6 and 7G7 as a pair of antibodies which had high affinity and recognized different epitopes located on separate structural domains of the toxin for ricin colorimetric sandwich ELISA detection. Anti-ricin B chain antibody 7G7 was used as the detection antibody, and anti-ricin A chain antibody 6A6 was used as the capture antibody. Using this pair of antibodies, the limits of detection (LOD) for ricin detection was 50 pM by conventional colorimetric sandwich ELISA (Fig. 2C).

3.3. Preparation of IDAM electrodes and nanoparticle probes

In order to enhance the sensitivity of ricin electrical detection, we used IDAMs as electrodes and nanoparticles as probes. In a typical experiment, IDAMs with five pairs of 300 μm wide, 4000 μm long gold electrodes separated by a gap of 100 μm were prepared by standard photolithography (Fig. 3A).

To assemble the SEIA we used two types of nanoparticles. GNPs, chosen because of their good catalytic and cooperative binding properties, have been widely applied for gene analysis, antigen or antibody detection (Taton et al., 2000). Transmission electron microscopy (TEM) showed that the GNPs had a diameter of 10 nm and appeared spherical and homogeneous (Fig. 3B). To know the efficiency of 7G7 modified on GNPs, Bradford protein concentration assay was used to determine the concentration of 7G7 in supernatant before and after conjugation. We found that nearly 100% 7G7 was conjugated on GNPs (data not shown). To detect whether the detection antibody still retained its bioactivity, we introduced ricin to the nitrocellulose membrane and used abrin as a negative control. After 5%

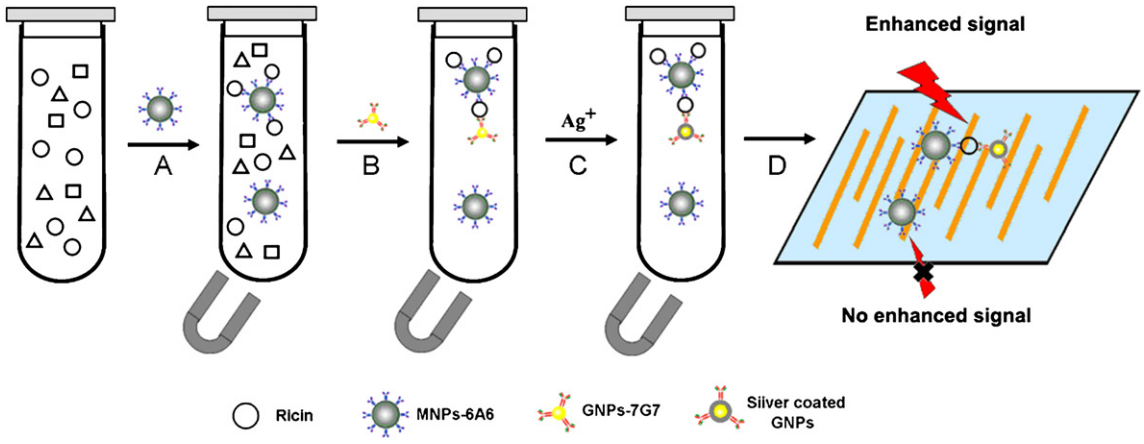

Fig. 1. Scheme of the silver enhancement immunoassay (SEIA) using IDAMs as electrodes for ricin electrical detection.

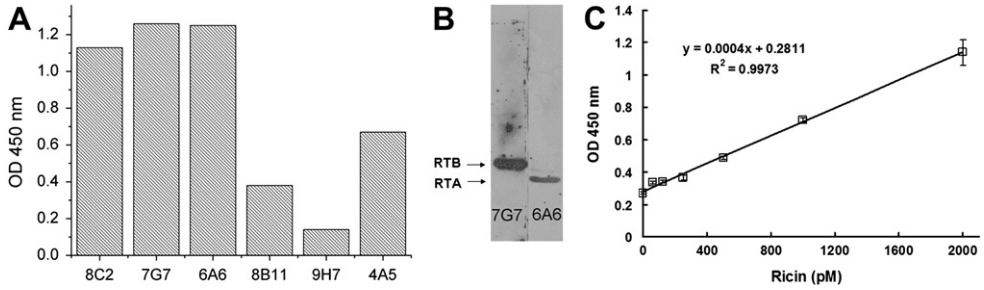

Fig. 2. Characterization of a panel of antibodies against ricin. (A) A panel of anti-ricin antibodies were bound to purified ricin. (B) Epitope mapping of two anti-ricin antibodies, 6A6 and 7G7, which possessed stronger binding activities than the other antibodies tested. The two domains of ricin were separated by reducing SDS-PAGE and recognized by the two anti-ricin antibodies. (C) Results of colorimetric sandwich ELISA for ricin detection. Anti-ricin B chain antibody 7G7 was used as the detection antibody, and anti-ricin A chain antibody 6A6 was used as the capture antibody. Using this pair of antibodies, the LOD for ricin detection was 50 pM. Error bars shown represent the standard error derived from three repeated measurements.

(w/v) milk blocking, the membrane was immersed into a solution containing detection antibody-coated GNPs. We could observe that GNP probes could be immobilised on the nitrocellulose membrane in the presence of ricin, but not abrin (see Supplementary information, Fig. S1).

MNPs are widely used because of their relatively easy separation properties which provided excellent target antigen enrichment. In the SEIA system, we used silica modified MNPs before immobilizing the antibody because peroxidase activity was minimized by shielding with silica (Gao et al., 2007). The size and shape of MNPs were examined by TEM and shown to be spherical and homogeneous (Fig. 3C). The catalytic properties of MNPs without silica coated and silica modified MNPs were compared using TMB as substrate in the presence of H_2O_2, with maximum absorbance at 652 nm. As shown in Supplementary information, Fig. S2, the silica coated MNPs had no peroxidase activity, showing that the silica modification shielded the peroxidase activity of MNPs. Then, 1 μm MNPs with a magnetic iron oxide core and a carboxyl-modified silica coating, were functionalized with capture antibody. Using the Bradford protein concentration assay, more than 80% capture antibody was conjugated on MNPs (data not shown). The bioactivity of capture antibody on MNPs was detected using the same method as for GNPs probes (see Supplementary information, Fig. S3), which showed that the MNPs were well coated with capture antibody.

3.4. Formation of the sandwich structure

Microscopic images and scanning electron microscope (SEM) observations were used to confirm the formation of the sandwich structure of the MNP–capture antibody–ricin–GNP–detection antibody and the amplification of electrical signal through silver enhancement. Microscopic observations after silver enhancement showed that MNPs from ricin-containing samples were heavily darkened relative to controls (Fig. 4A and B), due to the large number of GNPs that had triggered silver deposition. SEM observations of particulate bridges demonstrated that only the MNPs from experimental groups formed sandwich clusters (Fig. 4D). In the absence of ricin, the sandwich structure was not found and SEM images did not identify any GNPs that had bound to MNPs (Fig. 4C). These results indicated that MNP–capture antibody–ricin–GNP–detection antibody–silver particle complex was successfully formed in the presence of ricin.

3.5. Specificity of silver enhancement immunoassay for electrical detection of ricin toxin

Due to the excellent conductivity of Ag compared with MNPs there is a marked change in the resistance between the electrodes causing an enhancing electrical measurement. The resistance of each experiment was measured

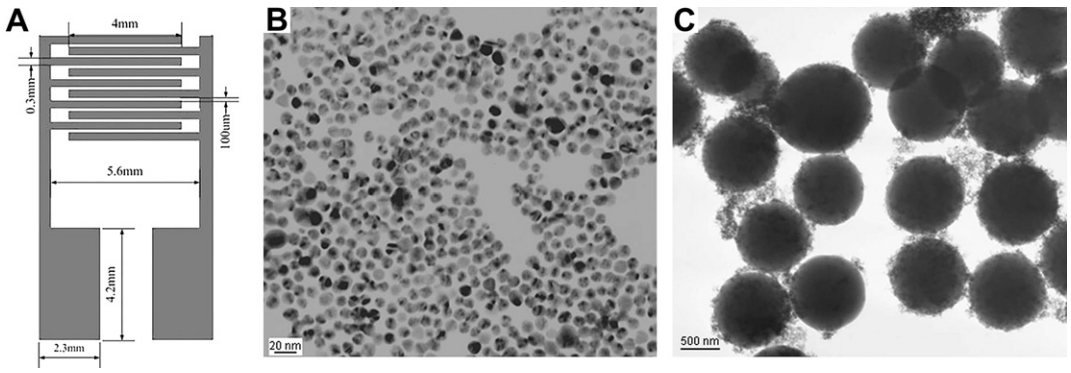

Fig. 3. (A) Diagram of the IDAMs with five pairs of 300 μm wide, 4000 μm long gold electrodes separated by a gap of 100 μm. TEM images of GNPs (B) and MNPs (C). The diameters of the GNPs and MNPs were approximately 10 nm and 1 μm, respectively.

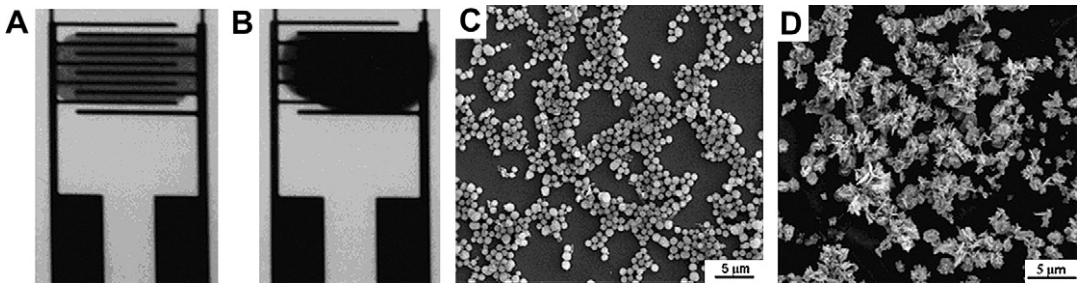

Fig. 4. Microscope (A, B) and SEM images (C, D) of the sandwich structure formation. Microscope images of ricin-containing samples (B) were heavily darkened relative to controls (A). SEM observations of particulate bridges demonstrated that MNPs from experimental groups (D) formed sandwich clusters whilst control MNPs did not (C).

using a Fluke 189 multimeter which is suitable for disposable assays. A marked electrical response, a resistance of about 210 Ω, was detected in the presence of 0.1 nM ricin toxin. In contrast, no enhanced electrical response above 20,000 Ω was observed for negative controls (Fig. 5). Comparing to the negative control groups, there was almost two orders of magnitude decrease of resistance in the presence of ricin which was a marked enhancement of electrical signal and could indicate the existence of ricin. When MNPs labeled with non-specific mIgG were used instead of anti-ricin antibody 7G7, the MNPs labeled with non-specific mIgG failed to give rise to any enhancing electrical signal whose resistance was around 28,000 Ω. This result confirmed the specific binding of 7G7 and 6A6 to ricin. On the other hand, we also used abrin to assess the specificity of this assay, no electrical signal was observed in the presence of abrin (Fig. 5A).

3.6. Effect of the enrichment property of MNPs on the sensitivity of SEIA

The SEIA system was developed by employing magnetic property of MNPs, where the magnetic property was used to capture, separate, and enrich the antigen in the sample prior to the assay process. Many previous studies have reported that MNPs have been used to enrich the target and enhance the detection sensitivity (Font et al., 2008). The enrichment property of MNPs was evaluated for its ability to detect 0.1 nM ricin in different volumes of detection system (200 and 1000 μl). As expected, one order of magnitude reduction of resistance was obtained in a volume of 1000 μl, with greater resistance in 200 μl detection system (Fig. 5B). These results indicated that the MNPs could successfully enrich the target and enhance the system sensitivity.

3.7. Detection sensitivity and reproducibility of the silver enhancement immunoassay for electrical detection of ricin toxin

Sensitivity of this system was assessed by monitoring the dependence of the electrical signal on the concentration of ricin toxin. The resistance of the electrode was constantly low with decreasing ricin concentration down to 10^{-11} M and then jumped up to become above 20,000 Ω for a ricin concentration of about 10^{-12} M or less. Thus, we took the

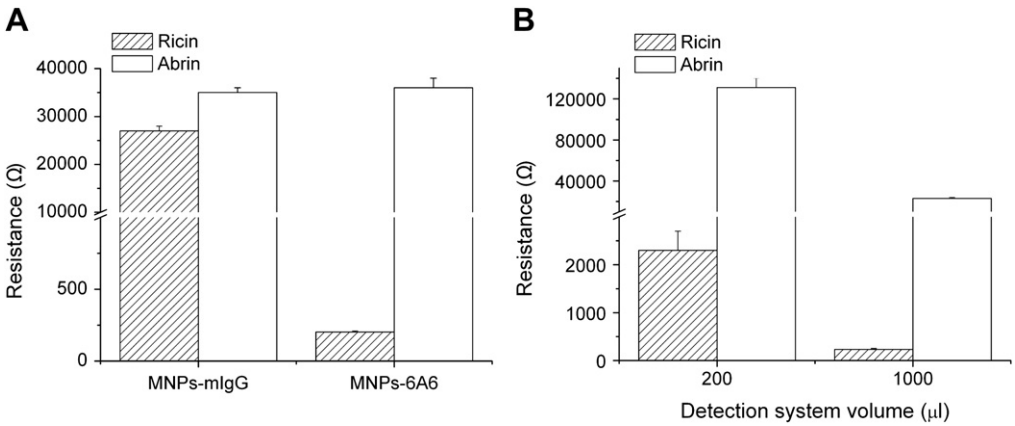

Fig. 5. (A) The specificity of SEIA using IDAMs as electrodes for ricin electrical detection. A marked electrical signal was observed in the presence of 0.1 nM ricin, but no electrical response was observed for abrin. MNPs labeled with non-specific mIgG failed to cause any electrical signal. (B) Effect of the enrichment property of MNPs on the sensitivity of SEIA. The MNPs could successfully enrich the target and enhance the electrical signal. Error bars shown represent the standard error derived from three repeated measurements.

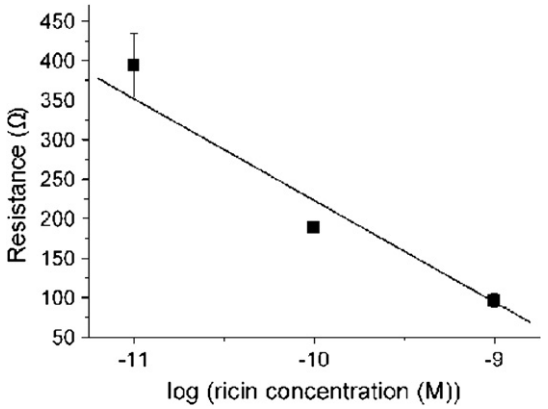

Fig. 6. The sensitivity of SEIA using IDAMs as electrodes for ricin electrical detection. A marked electrical signal was observed when ricin concentration was above 10 pM. Error bars shown represent the standard error derived from three repeated measurements.

LOD of our model sensors as 10^{-11} M. A marked electrical signal was observed when ricin concentration was greater than 10^{-11} M. All positive sensors had a resistance of less than 1000 Ω, while the resistance of the electrode pairs in the negative controls was above 20,000 Ω (Fig. 6). Compared with colorimetric sandwich ELISA using the same pair of antibodies, the sensitivity and time required for these two techniques was compared and results are shown in Table 1. The LOD of the SEIA was about 5 times lower than colorimetric sandwich ELISA, demonstrating that SEIA had a greater sensitivity than colorimetric sandwich ELISA. The enhanced sensitivity may be contributed to GNPs initiating silver deposition, and deposited silver further catalyzing silver reduction which can lead to a five orders of magnitude improvement in the sensitivity of detection (Park et al., 2002). As a result, the sensitivity of our system for ricin detection was greater than conventional ELISA. Furthermore, once detection antibody was coated on the plates or MNPs, the conventional colorimetric sandwich ELISA took 3 h, while the SEIA took less than 1 h. This may be due to the fact that a diffusion barrier that significantly reduces the reaction rate was formed. Thus from a kinetics point of view, solution phase reactions are preferable to solid phase reactions as they may reduce the hybridization time (Soderlund, 1990).

Assay reproducibility was assessed by examining the variation in signal at several ricin concentrations (each with two independent assays). The coefficients of variation (CV) across all ricin concentrations tested were less than 20% (Table 2), demonstrating that SEIA system have the comparable reproducibility as conventional ELISA (Table 1).

Table 1
Comparison of methods developed for ricin detection.

Ricin detection method	Sensitivity (pM)	Time taken (h)	Coefficient of variation (%)
Conventional ELISA	50	3	2.3–15.9
SEIA	10	1	8.9–18.8

Table 2
SEIA reproducibility evaluation.

Ricin (pM)	Resistance (Ω)		Coefficient of variation (%)
	1st	2nd	
1000	107	86	8.88
100	220	157	13.64
10	510	319	18.81

4. Conclusions

An ultrasensitive SEIA with IDAMs as electrodes for ricin detection is reported. In this system, a sandwich structure of MNP–capture antibody–ricin–GNP–detection antibody was formed. Then the GNPs performed silver reduction giving rise to an enhanced electrical signal. This method can specifically detect as little as picomolar concentrations of ricin. We have shown that our SEIA for ricin electrical detection is more rapid, sensitive and convenient than conventional colorimetric sandwich ELISA for ricin detection. This new system can be extended to detect target molecules with matched antibodies and has potential applications for many other toxin and virus detection.

Acknowledgments

This work was partially supported by grants from the National Natural Science Foundation of China (30672436), the Knowledge Innovation Program of the Chinese Academy of Sciences (KSCX2-YW-R-121, KSCX2-YW-G-044, KJCX2-YW-nano02), the Chinese Ministry of Sciences Project (2006AA02A245, 2006CB910901, 2006CB933204, 2006CB933300, 2009CB521700, 2008ZX10004-005, 2008 ZX10002-017) and the Ministry of Education, Culture, Sports, Science and Technology of Japan for Program of Founding Research Centers for Emerging and Reemerging Infectious Diseases.

We thank Ruimin Zheng and Xudong Zhao from the IBP core facilities centre for the technical support.

Conflict of interest

The authors have no conflict of interest.

Appendix. Supplementary information

Supplementary data associated with this article can be found in the online version, at doi:10.1016/j.toxicon.2009.07.015.

References

Alexiou, C., Jurgons, R., Seliger, C., Brunke, O., Iro, H., Odenbach, S., 2007. Delivery of superparamagnetic nanoparticles for local chemotherapy after intraarterial infusion and magnetic drug targeting. Anticancer Research 27, 2019–2022.

Ao, L., Gao, F., Pan, B., He, R., Cui, D., 2006. Fluoroimmunoassay for antigen based on fluorescence quenching signal of gold nanoparticles. Analytical Chemistry 78, 1104–1106.

Atlas, R.M., 2002. Bioterriorism: from threat to reality. Annual Review of Microbiology 56, 167–185.

Berggren, C., Bjarnason, B., Johansson, G., 2001. Capacitive biosensors. Electroanalysis 13, 173–180.

Chemla, Y.R., Grossman, H.L., Poon, Y., McDermott, R., Stevens, R., Alper, M.D., Clarke, J., 2000. Ultrasensitive magnetic biosensor for homogeneous immunoassay. Proceedings of the National Academy of Sciences of the United States of America 97, 14268–14272.

Chertok, B., Moffat, B.A., David, A.E., Yu, F., Bergemann, C., Ross, B.D., Yang, V.C., 2008. Iron oxide nanoparticles as a drug delivery vehicle for MRI monitored magnetic targeting of brain tumors. Biomaterials 29, 487–496.

Elghanian, R., Storhoff, J.J., Mucic, R.C., Letsinger, R.L., Mirkin, C.A., 1997. Selective colorimetric detection of polynucleotides based on the distance-dependent optical properties of gold nanoparticles. Science (New York, N.Y.) 277, 1078–1081.

Fan, A., Lau, C., Lu, J., 2008. Colloidal gold–polystyrene bead hybrid for chemiluminescent detection of sequence-specific DNA. The Analyst 133, 219–225.

Fang, C., Fan, Y., Kong, J., Gao, Z., Balasubramanian, N., 2008. Electrical detection of oligonucleotide using an aggregate of gold nanoparticles as a conductive tag. Analytical Chemistry 80, 9387–9394.

Font, H., Adrian, J., Galve, R., Esevez, M.C., Castellari, M., Gratacos-Cubarsi, M., Sanchez-Baeza, F., Marcot, M.P., 2008. Immunochemical assays for direct sulfonamide antibiotic detection in milk and hair samples using antibody derivatized magnetic nanoparticles. Journal of Agricultural and Food Chemistry 56, 736–743.

Gao, L., Zhuang, J., Nie, L., Zhang, J., Zhang, Y., Gu, N., Wang, T., Feng, J., Yang, D., Perrett, S., Yan, X., 2007. Intrinsic peroxidase-like activity of ferromagnetic nanoparticles. Nature Nanotechnology 2, 577–583.

Garber, E.A., O'Brien, T.W., 2008. Detection of ricin in food using electrochemiluminescence-based technology. Journal of AOAC International 91, 376–382.

Godal, A., Olsnes, S., Pihl, A., 1981. Radioimmunoassays of abrin and ricin in blood. Journal of Toxicology and Environmental Health 8, 409–417.

Gu, H., Xu, K., Xu, C., Xu, B., 2006. Biofunctional magnetic nanoparticles for protein separation and pathogen detection. Chemical Communications (Cambridge, England), 941–949.

Guglielmo-Viret, V., Thullier, P., 2007. Comparison of an electrochemiluminescence assay in plate format over a colorimetric ELISA, for the detection of ricin B chain (RCA-B). Journal of Immunological Methods 328, 70–78.

Hill, H.D., Mirkin, C.A., 2006. The bio-barcode assay for the detection of protein and nucleic acid targets using DTT-induced ligand exchange. Nature Protocols 1, 324–336.

Hill, H.D., Vega, R.A., Mirkin, C.A., 2007. Nonenzymatic detection of bacterial genomic DNA using the bio bar code assay. Analytical Chemistry 79, 9218–9223.

Hoshino, A., Ohnishi, N., Yasuhara, M., Yamamoto, K., Kondo, A., 2007. Separation of murine neutrophils and macrophages by thermoresponsive magnetic nanoparticles. Biotechnology Progress 23, 1513–1516.

Kirby, R., Cho, E.J., Gehrke, B., Bayer, T., Park, Y.S., Neikirk, D.P., McDevitt, J.T., Ellington, A.D., 2004. Aptamer-based sensor arrays for the detection and quantitation of proteins. Analytical Chemistry 76, 4066–4075.

Kohler, G., Milstein, C., 1975. Continuous cultures of fused cells secreting antibody of predefined specificity. Nature 256, 495–497.

Narang, U., Anderson, G.P., Ligler, F.S., Burans, J., 1997. Fiber optic-based biosensor for ricin. Biosensors and Bioelectronics 12, 937–945.

Oliver, C., 1994. Preparation of colloidal gold. Methods in Molecular Biology (Clifton, N.J.) 34, 299–302.

Paguirigan, A.L., Beebe, D.J., 2007. Protocol for the fabrication of enzymatically crosslinked gelatin microchannels for microfluidic cell culture. Nature Protocols 2, 1782–1788.

Park, S.J., Taton, T.A., Mirkin, C.A., 2002. Array-based electrical detection of DNA with nanoparticle probes. Science (New York, N.Y.) 295, 1503–1506.

Poli, M.A., Rivera, V.R., Hewetson, J.F., Merrill, G.A., 1994. Detection of ricin by colorimetric and chemiluminescence ELISA. Toxicon 32, 1371–1377.

Roberts, L.M., Smith, D.C., 2004. Ricin: the endoplasmic reticulum connection. Toxicon 44, 469–472.

Soderlund, H., 1990. DNA hybridization: comparison of liquid and solid phase formats. Annales de biologie clinique 48, 489–491.

Stine, R., Pishko, M.V., Schengrund, C.L., 2005. Comparison of glycosphingolipids and antibodies as receptor molecules for ricin detection. Analytical Chemistry 77, 2882–2888.

Taton, T.A., Lu, G., Mirkin, C.A., 2001. Two-color labeling of oligonucleotide arrays via size-selective scattering of nanoparticle probes. Journal of the American Chemical Society 123, 5164–5165.

Taton, T.A., Mirkin, C.A., Letsinger, R.L., 2000. Scanometric DNA array detection with nanoparticle probes. Science (New York, N.Y.) 289, 1757–1760.

Tran, H., Leong, C., Loke, W.K., Dogovski, C., Liu, C.Q., 2008. Surface plasmon resonance detection of ricin and horticultural ricin variants in environmental samples. Toxicon 52, 582–588.

Varshney, M., Li, Y., 2007. Interdigitated array microelectrode based impedance biosensor coupled with magnetic nanoparticle–antibody conjugates for detection of *Escherichia coli* O157:H7 in food samples. Biosensors and Bioelectronics 22, 2408–2414.

Varshney, M., Li, Y., 2008. Double interdigitated array microelectrode-based impedance biosensor for detection of viable *Escherichia coli* O157:H7 in growth medium. Talanta 74, 518–525.

Yang, H.H., Zhang, S.Q., Chen, X.L., Zhuang, Z.X., Xu, J.G., Wang, X.R., 2004. Magnetite-containing spherical silica nanoparticles for biocatalysis and bioseparations. Analytical Chemistry 76, 1316–1321.